Rare Metal Materials and Engineering
Volume 55, Issue 3, March 2026
Available online at www.rmme.ac.cn

Science Press

Cite this article as: Tian Zhenyun, Chen Jiawen, Zhang Run, et al. Thermodynamics of Reduction of Titania by CH_4-H_2 Gas Mixture[J]. Rare Metal Materials and Engineering, 2026, 55(03): 615-626. DOI: https://doi.org/10.12442/j.issn.1002-185X.20250147.

ARTICLE

Thermodynamics of Reduction of Titania by CH_4-H_2 Gas Mixture

Tian Zhenyun[1], Chen Jiawen[1], Zhang Run[1], Fan Gangqiang[1,2,3], Qiu Guibao[1,4]

[1] College of Materials Science and Engineering, Chongqing University, Chongqing 400044, China; [2] Chongqing Wangbian Electric (Group) Co., Ltd, Chongqing 401254, China; [3] Chongqing Key Laboratory of High Performance Oriented Electrical Steel, Chongqing 401254, China; [4] Chongqing Key Laboratory of Vanadium-Titanium Metallurgy and New Materials, Chongqing University, Chongqing 400044, China

Abstract: Given the considerable global interest in the preparation of Ti and TiC, a novel reduction method for TiO_2 in a CH_4-H_2 atmosphere was proposed, and the reduction thermodynamic behavior, phase equilibrium, and energy consumption of TiO_2 during its reaction with a CH_4-H_2 gas mixture were investigated. The results indicate that the reaction proceeds via a stepwise reduction pathway from TiO_2 to Ti(C, O), with the Magnéli phase (Ti_nO_{2n-1}) and Ti_3O_5 serving as intermediate phases. Notably, the reduction of TiO_2 by H_2 is more challenging than that by CH_4, which may be attributed to the inhibitory effect of H_2 on the surface carbon precipitation. For the complete carbonization of 1 mol TiO_2, the total energy required at 1000, 1100, and 1200 ℃ is 1159, 925, and 977 kJ/mol, respectively, which may be related to the shift of gas-phase equilibrium and the increase in side reactions at high temperatures.

Key words: TiO_2; TiC_xO_y; reduction-carbonization; thermodynamic behavior; energy consumption

1 Introduction

Titanium and its alloys are noted for their unique combination of properties, including high strength, low density, a high melting point, excellent corrosion resistance, and superior biocompatibility[1–8], making them essential in aerospace, defense, biomedicine, and daily-life applications[9-13]. The history of titanium metal preparation dates back to the 1910s, when Hunter synthesized Ti from $TiCl_4$ using sodium as a reductant in a steel reactor filled with argon gas[14]. However, the early method for producing sponge titanium suffered from restrictions such as high impurity levels and low efficiency, leading to its replacement by the Kroll method, developed in the 1950s, which offered enhanced efficiency[15–17]. The Kroll method involves two key steps: first, the carbothermal chlorination of TiO_2 to produce $TiCl_4$; second, the reaction of $TiCl_4$ with liquid Mg to yield metallic titanium. The resulting product then undergoes vacuum distillation to remove impurities, ultimately obtaining sponge titanium with low oxygen content[18–19]. Despite cost reduction benefits, the Kroll method still faces challenges like high energy consumption during the carbothermal chlorination step and equipment corrosion caused by chlorine gas at high temperatures[20–22].

In titanium production, extensive efforts have been devoted to find more efficient processes than the Kroll method, aiming to lower costs and enhance energy efficiency. Researchers at Pangang Group Research Institute Co., Ltd have worked on titanium-containing blast furnace slag: they first generated TiC and TiC_xO_y via a carbothermal reaction; then, these products are subjected to selective chlorination to produce $TiCl_4$; finally, $TiCl_4$ was reduced to sponge titanium via a magnesiothermic process. This approach improves the utilization of low-grade titanium resources and lowers production costs[23–24]. In the 1950s, the MER Corporation developed a process that uses cheap titanium feedstocks and a carbon composite anode. This process releases Ti ions into the electrolyte during electrolysis, and then they are deposited as solid Ti on the cathode[25]. Later, in 1991, Popov et al[26] used TiC as a consumable anode for the cathodic deposition of high-purity titanium; however, this method also generates Magnéli phases and carries the risk of carbon contamination

Received date: March 19, 2025
Corresponding author: Fan Gangqiang, Ph. D., College of Materials Science and Engineering, Chongqing University, Chongqing 400044, P. R. China, E-mail: fangangqiang@cqwbdq.com; Qiu Guibao, Ph. D., Professor, College of Materials Science and Engineering, Chongqing University, Chongqing 400044, P. R. China, E-mail: qiuguibao@cqu.edu.cn

in the final product. The USTB process, developed by the University of Science and Technology Beijing, starts by reducing TiO_2 with carbon to produce electrically conductive TiC_xO_y, which is then used as an anode in electrolysis to release low-valent Ti ions into the molten salt, ultimately forming pure Ti at the cathode[27–28].

These innovative approaches, which use TiC and TiC_xO_y as raw materials for titanium production, demonstrate new advancements in the field towards cost reduction and efficiency enhancement. These methods not only lessen the environmental impact but also improve the production efficiency and quality of Ti materials. The primary method for producing TiC/TiC_xO_y is the carbothermal reduction process, which employs TiO_2 powder and carbon powder as raw materials in a high-temperature argon atmosphere. Although this method is cost-effective and simple, it is associated with high energy consumption and substantial carbon emissions[29]. Additionally, for the production of high-purity TiC, Feng et al[30–31] suggested the synthesis of TiC nanoparticles through an 8 h reaction between $TiCl_4$ and CaC_2 at 500 ℃ under high-pressure conditions. Wang et al[32] proposed a process that combines TiO_2 with CaC_2/$NaNH_2$, supplemented by metallic magnesium under high pressure, to produce TiC. These processes typically employ high-purity TiO_2 powder and $TiCl_4$ as raw materials, both of which are costly. Moreover, the complexity of these processes and the high energy consumption during production restrict their application to only the manufacturing of materials with specific requirements.

To address these challenges, a novel reduction approach using CH_4 is proposed as an alternative to traditional high-temperature carburization techniques. Previous research has demonstrated the successful synthesis of TiC using methane-bearing gas[33–35]. Subsequently, an innovative process aimed at reducing TiO_2 with a CH_4-H_2 gas mixture has shown considerable potential advantages and has been deemed feasible, confirming that TiO_2 can be reduced and carbonized to Ti(C, O) under a CH_4-H_2 atmosphere at relatively low temperatures[36–37]. However, the reduction products of TiO_2 reduced by H_2 and CH_4 are relatively complex, containing not only water and carbon dioxide but also solid solutions and low-valent titanium oxides. The formation of these products is influenced by system pressure, gas composition, and reaction temperature[38–41]. Hence, the reactions between TiO_2 and the CH_4-H_2 gas mixture during the reduction process are markedly more complicated. To decipher the reaction stages and energy consumption of this novel process, this study explored the thermodynamic behavior of TiO_2 under a CH_4-H_2 atmosphere and estimated the reaction enthalpy changes.

2 Experiment

2.1 Equilibrium composition calculation settings

The thermodynamic equilibrium and Gibbs free energy changes associated with the reduction of TiO_2 by a CH_4-H_2 gas mixture were calculated using FactSage 8.0, with the FactPS and FToxid databases used as data support. Initially, the reaction module was employed to compute all potential reactions between TiO_2 and the CH_4-H_2 gas mixture, with the consideration of the effects of different reaction pressures. Subsequently, the thermodynamic equilibrium of the system under various temperatures was determined using the equilibrium module, which is based on the principle of minimum Gibbs free energy. Additionally, the phase diagram module was used to generate the phase diagrams that illustrate the evolution of TiO_2 behavior with varying gas composition.

The initial and equilibrium states of the system are depicted in Fig. 1, while the initial gas volume fraction is detailed in Table 1. The reaction system contains both solid and gaseous phases. The reaction temperatures were set in the range from 900 ℃ to 1200 ℃ at intervals of 100 ℃. The system pressure was maintained constant before and after the reaction. To ensure the complete reduction and carbonization of TiO_2, the total reaction gas volume was set at 50 mol.

In practical industrial scenarios, a piston flow reactor configuration is often employed, where the reaction gas and solid reactants flow in countercurrent directions. This design enables the spent gas to rapidly depart from the reaction interface, while fresh reaction gas is immediately supplied to the interface. Thermodynamic calculations were conducted for an open system to determine the phase transformations and solid-phase composition. The reaction process was simulated through 1000 reaction steps, with each step introducing a fresh batch of 0.05 mol reaction gas.

2.2 Calculation of reaction enthalpy

The thermodynamic equilibrium of TiO_2 reacting with a CH_4-H_2 gas mixture was assessed in an open system to derive crucial information, including the composition of solid products and off-gas, along with the required amount of reducing gas. Based on these results, the change in reaction enthalpy was determined, which stemmed from the disparity

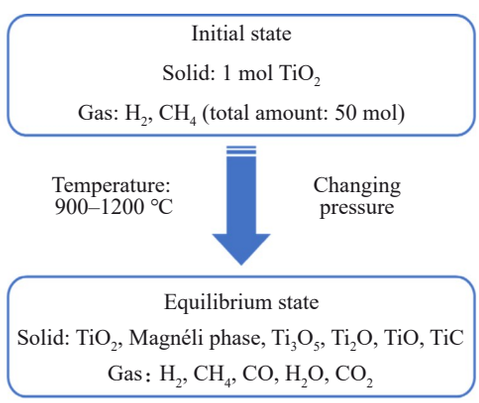

Fig.1 Initial and equilibrium states of reaction system

Table 1 Contents of initial reaction gases (vol%)

Order	CH_4	H_2	Total
(1)	4	96	100
(2)	8	92	100
(3)	12	88	100
(4)	16	84	100

in absolute enthalpy between reactants and products.

The enthalpy of a substance at a given state is an absolute value, which is derived from the fundamental data of ΔH_{298} and $C_p(T)$, as illustrated in Eq.(1–2).

$$H_T = \Delta H_{298} + \int_{298}^{T} C_p(T)\mathrm{d}T \quad (1)$$

$$C_p(T)=A_1+A_2\times10^{-3}T+A_3\times10^{5}T^{-2}+A^{4}\times10^{-6}T \quad (2)$$

where $C_p(T)$ denotes the isobaric molar heat capacity at a specific temperature T, with the unit of J/(mol·K); H_T denotes the standard molar enthalpy at temperature T, with the unit of J/mol; A_1, A_2, A_3, and A_4 are parameters characterizing the specific heat capacity; ΔH_{298} denotes the standard enthalpy change for formation of each substance at 298 K.

The enthalpy change of a chemical reaction denotes the heat absorbed or released by the system when the reaction reaches equilibrium. It is calculated as the difference between the total enthalpies of the products and those of the reactants, as delineated in Eq.(3).

$$\Delta H = \sum_{i=1}^{N} n_i H_{i,T_i} - \sum_{j=1}^{M} n_j H_{j,T_j} \quad (3)$$

where ΔH denotes the enthalpy change of reactions (kJ/mol), with a negative value indicating the exothermic reaction and a positive value indicating the endothermic reaction; indices i and j represent the components after and before the state change, respectively; N and M denote the number of components after and before the state change, respectively; n_i and n_j are the molar amounts of the components after and before the state change, respectively, with the unit of mol; T_i and T_j signify the thermodynamic temperatures of the components after and before the state change, respectively, and their units are K. The standard molar enthalpy of component i at temperature T_i and that of component j at temperature T_j are represented as $H_i^0(T_i)$ and $H_j^0(T_j)$, respectively, with the unit of kJ/mol.

3 Results and Discussion

3.1 Gibbs free energy change of reactions

The reduction and carbonization of TiO_2 is regarded as a stepwise process, with the phase transition sequence given as follows[42]:

$$TiO_2 \rightarrow \text{Magnéli}\,(Ti_nO_{2n-1}, n \geqslant 4) \rightarrow Ti_3O_5 \rightarrow Ti_2O_3 \quad (4)$$

The reaction of an ideal gas can be described by the following equation:

$$aA + bB = dD + hH \quad (5)$$

The Gibbs free energy change ΔG of this reaction is calculated by the following equation:

$$\Delta G = \Delta G^0 + \ln\left(\frac{p_D^d p_H^h}{p_A^a p_B^b} p^{\Theta\sum \mathrm{vi}}\right) \quad (6)$$

where ΔG^0 indicates the standard Gibbs free energy change. When the reaction gas is at standard atmospheric pressure, the following relationship holds:

$$\Delta G = \Delta G^0 \quad (7)$$

The possible reactions of TiO_2 with CH_4 and H_2 are listed in Table 2. The Gibbs free energy changes of TiO_2 in the presence of a CH_4-H_2 gas mixture were calculated using the Reaction Module of FactSage. Additionally, the relationship between Gibbs free energy changes and temperature, as well as the initial reaction temperature ($T_{initial}$) for each reaction, are identified and also shown in Table 2. The thermodynamic data

Table 2 Possible reactions of TiO_2 with CH_4 and H_2

Reaction	Equation	ΔG^0/kJ·mol^{-1}	$T_{initial}$/K
$20TiO_2+H_2=Ti_{20}O_{39}+H_2O$	Eq.(8)	120.446–0.063T	1919
$20TiO_2+CH_4=Ti_{20}O_{39}+CO+2H_2$	Eq.(9)	343.038–0.314T	1093
$10TiO_2+H_2=Ti_{10}O_{19}+H_2O$	Eq.(10)	120.007–0.057T	2088
$10TiO_2+CH_4=Ti_{10}O_{19}+CO+2H_2$	Eq.(11)	342.663–0.309T	1111
$9TiO_2+H_2=Ti_9O_{17}+H_2O$	Eq.(12)	119.993–0.057T	2112
$9TiO_2+CH_4=Ti_9O_{17}+CO+2H_2$	Eq.(13)	342.584–0.308T	1112
$8TiO_2+H_2=Ti_8O_{15}+H_2O$	Eq.(14)	120.002–0.056T	2140
$8TiO_2+CH_4=Ti_8O_{15}+CO+2H_2$	Eq.(15)	342.594–0.307T	1115
$7TiO_2+H_2=Ti_7O_{13}+H_2O$	Eq.(16)	120.146–0.055T	2173
$7TiO_2+CH_4=Ti_7O_{13}+CO+2H_2$	Eq.(17)	342.737–0.307T	1119
$6TiO_2+H_2=Ti_6O_{11}+H_2O$	Eq.(18)	120.506–0.054T	2218
$6TiO_2+CH_4=Ti_6O_{11}+CO+2H_2$	Eq.(19)	343.097–0.305T	1123
$5TiO_2+H_2=Ti_5O_9+H_2O$	Eq.(20)	121.316–0.053T	2278
$5TiO_2+CH_4=Ti_5O_9+CO+2H_2$	Eq.(21)	343.908–0.304T	1130
$4TiO_2+H_2=Ti_4O_7+H_2O$	Eq.(22)	123.168–0.052T	2360
$4TiO_2+CH_4=Ti_4O_7+CO+2H_2$	Eq.(23)	345.759–0.303T	1140
$3Ti_4O_7+H_2=4Ti_3O_5+H_2O$	Eq.(24)	172.077–0.071T	2427
$3Ti_4O_7+CH_4=4Ti_3O_5+CO+2H_2$	Eq.(25)	393.339–0.323T	1218
$2Ti_3O_5+H_2=3Ti_2O_3+H_2O$	Eq.(26)	119.044–0.003T	35407
$2Ti_3O_5+CH_4=3Ti_2O_3+CO+2H_2$	Eq.(27)	341.576–0.254T	1343
$Ti_2O_3+H_2=2TiO+H_2O$	Eq.(28)	180.893–0.024T	7610
$Ti_2O_3+CH_4=2TiO+CO+2H_2$	Eq.(29)	400.719–0.273T	1465
$Ti_2O_3+5CH_4=2TiC+3CO+10H_2$	Eq.(30)	123.675–1.042T	1186

ΔG_f^0 used in these calculations are shown in Table 3.

Meanwhile, the relationship between the Gibbs free energy change and temperature is illustrated in Fig. 2. It is evident that, except for Eq. (4), the initial reaction temperature for most reactions between titanium oxides and H_2 exceeds 2000 K (Fig. 2a and 2c), indicating that these reactions are relatively difficult to initiate. In contrast, the initial reaction temperature range for the reactions between titanium oxides and CH_4 is 1101–1147 K (Fig. 2b and 2d), suggesting that the reaction of TiO_2 with CH_4 occurs more readily.

The abovementioned calculations are based on the reactions occurring under standard atmospheric pressure conditions. In actual experiments, gaseous products are promptly removed along with the carrier gas, leading to a reduction in their partial pressures. Therefore, it is essential to investigate how the partial pressure of these gaseous products affects the reactions. For simplification, the transformation of TiO_2 to the Magnéli phase is represented by the reaction of TiO_2 to Ti_4O_7. Based on Eq. (6), the Gibbs free energy change of the reaction and temperature under varying partial pressures of gaseous products were calculated, with the result shown in Table 4.

Fig. 3 reflects the relationships between the Gibbs free energy change and the partial pressure of gaseous products under different temperatures. It is apparent that the Gibbs free energy change decreases when the temperature drops or the partial pressure of gaseous products decreases. Similarly, the initial reaction temperature declines sharply with the decrease in partial pressure. For the same phase transition stage, reactions involving CH_4 occur at a lower temperature than those involving H_2, indicating that CH_4 is thermodynamically

Table 3 Thermodynamic data (ΔG_f^0) of substances

Substance	ΔG_f^0/J·(mol·K)$^{-1}$
TiO_2	$-976986.65+484.74T+1683920.51T^{-1}-67156788.7T^{-2}-77.84T\ln(T)$
CH_4	$-348252.33+2678.16T+9.39\times10^{-3}T^2+2096686.07T^{-1}-67156788.7T^{-2}+110598.4\ln(T)-40575.91T^{0.5}-304.93T\ln(T)$
H_2	$-13779.82-17.72T-1.54\times10^{-3}T^2+147589.949T^{-1}-2.38\times10^{-7}T^3+779.44T^{0.5}-19.83T\ln(T)$
$Ti_{20}O_{39}$	$-19093826.9+10248.7T+28202486.3T^{-1}-8443.57T^{0.5}-1050417119T^{-2}-1609.77T\ln(T)$
$Ti_{10}O_{19}$	$-9324334.79+5406.56T+11363282T^{-1}-8443.57T^{0.5}-348849297T^{-2}-831.39T\ln(T)$
Ti_9O_{17}	$-8347427.08+4922.51T+9679361.2T^{-1}-8443.57T^{0.5}-311692519T^{-2}-753.56T\ln(T)$
Ti_8O_{15}	$-7370431.09+4438.51T+7995440T^{-1}-8443.57T^{0.5}-244535742T^{-2}-675.72T\ln(T)$
Ti_7O_{13}	$-6393300.79+3954.56T+6311520.07T^{-1}-8443.57T^{0.5}-177378958T^{-2}-597.88T\ln(T)$
Ti_6O_{11}	$-5415954.60+3470.77T+4627599.60T^{-1}-8443.57T^{0.5}-110222187T^{-2}-520.04T\ln(T)$
Ti_5O_9	$-4438156.96+2987.12T+2943679.14T^{-1}-8443.57T^{0.5}-43075407.1T^{-2}-442.2T\ln(T)$
Ti_4O_7	$-3459318.88+2503.43T+1259758.59T^{-1}-8443.57T^{0.5}+24091372.3T^{-2}-364.37T\ln(T)$
Ti_3O_5	$-2462333.91+1974.08T-3568008.3T^{-1}-8443.57T^{0.5}+353266752T^{-2}-278.9T\ln(T)$
Ti_2O_3	$-1171154.54+6399.42T-9404192.70T^{-1}-58419.46T^{0.5}-730.23T\ln(T)$
TiO	$-558169.7+25548T-8.9\times10^{-3}T^2+327010.59T^{-1}+1.1\times10^{-8}T^3-41.99T\ln(T)$ (α, 298–2500 K) $-553971.14+252.16T-8.9\times10^{-3}T^2+327074.65T^{-1}+1.1\times10^{-8}T^3-41.99T\ln(T)$ (β, 298–2500 K)
TiC	$-207428.36+348.26T-1.56\times10^{-3}T^2+2635236T^{-1}+1.07\times10^{-7}T^3-264300000T^{-2}+1.2\times10^{10}T^{-3}-53.36T\ln(T)$ (298–900 K) $-207180.25+347.63T-9.8\times10^{-4}T^2+2605280T^{-1}+9.09\times10^{-8}T^3-264300000T^{-2}+1.2\times10^{10}T^{-3}-53.36T\ln(T)$ (900–1155 K) $-198459.6+281.62T-4.92\times10^{-3}T^2+1084940T^{-1}+2.03\times10^{-7}T^3-264300000T^{-2}+1.2\times10^{10}T^{-3}-44.31T\ln(T)$ (1155–1941 K) $-323895.23+853.45T+1.14\times10^{-2}T^2+39262405T^{-1}+3.04\times10^{-7}T^3-264300000T^{-2}$ (1941–4000 K)
TiN	$-332270.49+457.36T+1.19\times10^{-2}T^2+332361.04T^{-1}-2.04\times10^{-6}T^3-5877.49\ln(T)-70.28T\ln(T)$(298–1100 K) $-347875.06+244.42T-4.9\times10^{-3}T^2-846809.02T^{-1}-40.76T\ln(T)$ (1100–3220 K)
H_2O	$-255475.808-15.17T-7.47\times10^{-3}T^2+13999.66T^{-1}+9.2\times10^{-8}T^3+1107.27\ln(T)-25.78T\ln(T)$ (298–1100 K) $-152152.281+164.81T-8.05\times10^{-5}T^2-12075583.2T^{-1}+5947.37T^{0.5}-83128.2757\ln(T)-53.15T\ln(T)$ (1100–4000 K)
CO	$-203680.54+609.46T+3.12\times10^{-3}T^2+770627.67T^{-1}-10357.02T^{0.5}+32063.3157\ln(T)-90.75T\ln(T)$
CO_2	$-415578.81+642.77T+2.37\times10^{-3}T^2+20124.52T^{-1}-6993.15T^{0.5}+11004.74\ln(T)-103.34T\ln(T)$
C	$20210.98+515.6T+4\times10^{-3}T^2-412784.99T^{-1}-4096.06T^{0.5}+1100795.94T^{-2}-61.18T\ln(T)$(298–1000 K) $-13835.85+176.4T-4.79\times10^{-4}T^2+1441704.16T^{-1}-158.77T^{0.5}-24.78T\ln(T)$ (1000–6000 K)

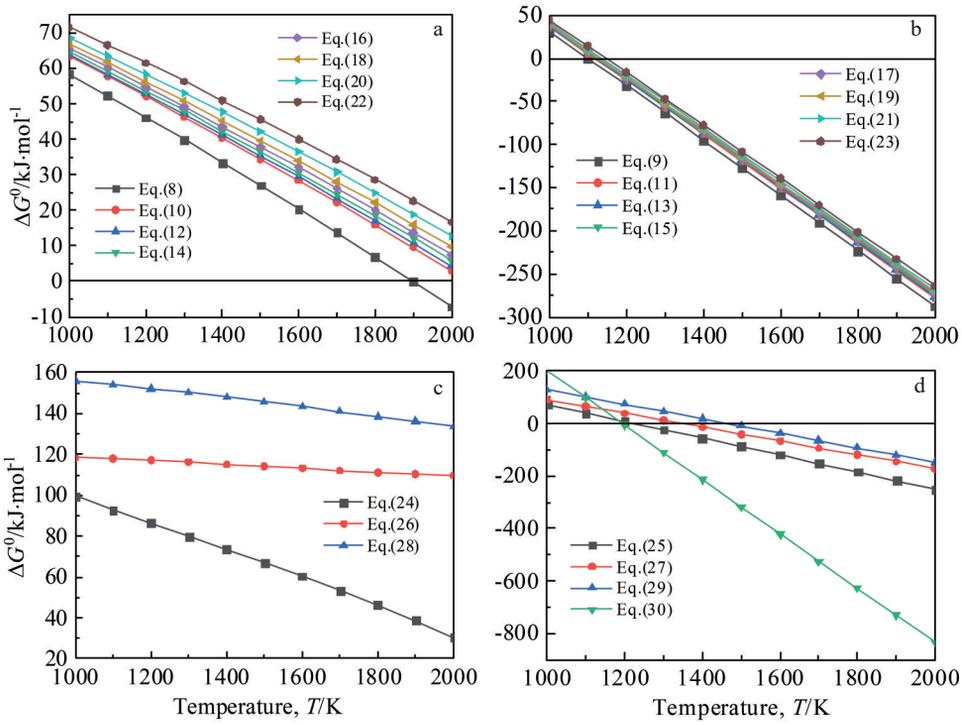

Fig.2 Relationships between standard Gibbs free energy change of Eq.(8–30) and temperature

beneficial to the reduction.

In industrial process, the operating pressure of the reactor ranges from 2×101 kPa to 4×101 kPa. Reactions have been calculated under different system pressures. Changes in system pressure do not affect the reactions involving H_2; therefore, only the reactions involving CH_4 are considered, with the results presented in Table 5 and Fig.4. The calculations demonstrate that an increase in system pressure impedes the reduction process, causing the initial reaction temperature to rise progressively.

3.2 Equilibrium phase diagram of TiO_2 in CH_4-H_2 system

The phase equilibrium of TiO_2 in a CH_4-H_2 system with varying gas composition is illustrated in Fig.5. As the quantity of reducing gas increases, TiO_2 is initially transformed into the Magnéli phase (Ti_nO_{2n-1}, $n\geqslant4$), followed by the Ti_3O_5 phase, and ultimately transformed into a solid solution phase Ti(C, O) composed of TiC and TiO. Additionally, solid carbon is deposited and coexists with titanium oxides at relatively low temperatures. With higher CH_4 concentrations in the gas mixture, the zone where the Ti(C, O) solid solution exists independently, as well as the region where the Ti(C, O) coexist with Ti_3O_5 shifts towards the area with a lower gas/TiO_2 molar ratio, indicating a reduced total gas requirement for the formation of Ti(C, O). This suggests that the reduction efficiency of titanium oxides is improved with increasing the CH_4 content.

3.3 Solid phase composition of TiO_2-CH_4-H_2 system

The TiO_2-(8vol% CH_4-92vol% H_2) system was analyzed at various temperatures, and the results are presented in Fig.6. It can be observed that TiO_2 is progressively reduced to the Magnéli phase and Ti_3O_5, and ultimately forms a Ti(C, O) solid solution. Notably, at 1173 K, Ti_4O_7, rather than Ti_3O_5, is directly transformed into the Ti(C, O) solid solution and cannot be fully reduced even with 50 mol gas. When the temperature exceeds 1373 K, the titanium oxides are entirely converted into the Ti(C, O) solid solution. Thus, an appropriate increase in reaction temperature positively influences the formation of the Ti(C, O) solid solution. As the temperature decreases, solid C is more likely to precipitate in conditions of lower gas partial pressure. In other words, at lower temperatures, methane gas adsorbed on the surface of TiO_2 is more prone to decomposition and generation of solid C. According to Ref.[32–33], C formed under these conditions exhibits excellent activity, enabling the reduction of TiO_2 at lower temperatures.

Fig.7a illustrates the amount of gas required for the initial and complete formation of the Ti(C, O) solid solution at various temperatures. It is observed that as the reaction temperature increases from 1173 K to 1473 K, the amount of gas required for the initial formation of the Ti(C, O) solid solution decreases from 8.1 mol to 3.4 mol, while the amount required for its complete formation decreases from 48.0 mol to 23.9 mol.

The contents of carbon and oxygen in the Ti(C, O) solid solution are crucial indicators of the deoxidation degree of titanium oxides. Fig. 7b depicts the change in TiC content within the Ti(C, O) solid solution relative to the gas/TiO_2 molar ratio at different temperatures. When the gas/TiO_2 molar ratio exceeds 23.9, the TiC concentration in the solid solution rises with increasing the gas content. The turning point of the TiC content aligns with the disappearance of Ti_3O_5

Table 4 Gibbs free energy change of titanium oxides reacting with CH_4-H_2 under different product partial pressures

Reaction	P_{H_2O} or P_{CO}/×101 kPa	ΔG/kJ·mol^{-1}	$T_{initial}$/K
$4TiO_2+H_2=Ti_4O_7+H_2O$	1	123.168–0.052T	2360
	10^{-1}	123.168–0.071T	1727
	10^{-2}	123.168–0.090T	1361
	10^{-3}	123.168–0.109T	1124
	10^{-4}	123.168–0.129T	957
$4TiO_2+CH_4=Ti_4O_7+CO+2H_2$	1	345.759–0.303T	1140
	10^{-1}	345.759–0.322T	1073
	10^{-2}	345.759–0.341T	1013
	10^{-3}	345.759–0.361T	958
	10^{-4}	345.759–0.380T	910
$3Ti_4O_7+H_2=4Ti_3O_5+H_2O$	1	172.077–0.071T	2427
	10^{-1}	171.980–0.090T	1908
	10^{-2}	171.884–0.109T	1572
	10^{-3}	171.788–0.128T	1337
	10^{-4}	171.691–0.148T	1162
$3Ti_4O_7+CH_4=4Ti_3O_5+CO+2H_2$	1	393.339–0.323T	1218
	10^{-1}	393.289–0.342T	1150
	10^{-2}	393.182–0.361T	1088
	10^{-3}	393.096–0.380T	1033
	10^{-4}	393.000–0.399T	984
$2Ti_3O_5+H_2=3Ti_2O_3+H_2O$	1	119.044–0.003T	35407
	10^{-1}	119.044–0.022T	5289
	10^{-2}	119.044–0.042T	2858
	10^{-3}	119.044–0.061T	1958
	10^{-4}	119.044–0.080T	1489
$2Ti_3O_5+CH_4=3Ti_2O_3+CO+2H_2$	1	341.576–0.254T	1343
	10^{-1}	341.576–0.273T	1249
	10^{-2}	341.576–0.393T	1167
	10^{-3}	341.576–0.311T	1096
	10^{-4}	341.576–0.331T	1032
$Ti_2O_3+H_2=2TiO+H_2O$	1	180.893–0.024T	7610
	10^{-1}	180682–0.043T	4220
	10^{-2}	180.471–0.062T	2918
	10^{-3}	180.261–0.081T	2228
	10^{-4}	180.050–0.100T	1802
$Ti_2O_3+CH_4=2TiO+CO+2H_2$	1	400.719–0.273T	1465
	10^{-1}	400.509–0.292T	1369
	10^{-2}	400.298–0.311T	1285
	10^{-3}	400.087–0.330T	1210
	10^{-4}	399.876–0.349T	1143
$Ti_2O_3+5CH_4=2TiC+3CO+10H_2$	1	123.675–1.042T	1186
	10^{-1}	123.643–1.099T	1124
	10^{-2}	123.611–1.157T	1068
	10^{-3}	123.580–1.215T	1017
	10^{-4}	123.549–1.273T	971

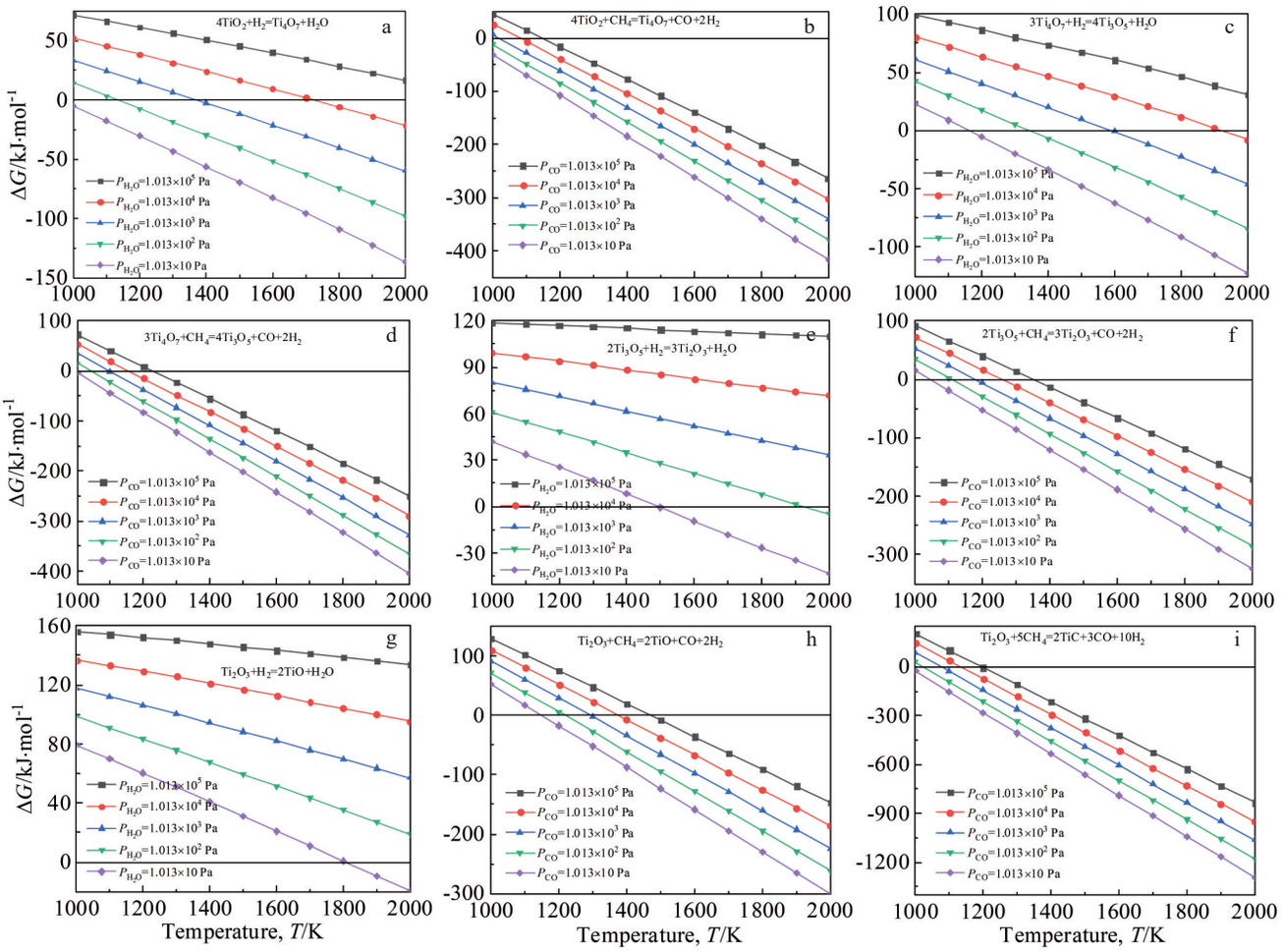

Fig.3 Relationships between Gibbs free energy change and temperature under different partial pressures of gaseous products

Table 5 Gibbs free energy change for reactions of titanium oxides with a CH_4-H_2 gas mixture under varying system pressures

Reaction	P/×101 kPa	ΔG/kJ·mol^{-1}	$T_{initial}$/K
$4TiO_2+CH_4=Ti_4O_7+CO+2H_2$	1	354.759–0.303T	1140
	2	354.759–0.292T	1185
	3	354.759–0.285T	1213
	4	354.759–0.280T	1234
$3Ti_4O_7+CH_4=4Ti_3O_5+CO+2H_2$	1	394.992–0.322T	1228
	2	394.992–0.310T	1274
	3	394.992–0.303T	1302
	4	394.992–0.299T	1323
$2Ti_3O_5+CH_4=3Ti_2O_3+CO+2H_2$	1	341.576–0.254T	1343
	2	341.576–0.243T	1407
	3	341.576–0.236T	1447
	4	341.576–0.231T	1477
$Ti_2O_3+CH_4=2TiO+CO+2H_2$	1	403.743–0.275T	1469
	2	403.743–0.263T	1533
	3	403.743–0.257T	1573
	4	403.743–0.252T	1603
$Ti_2O_3+5CH_4=2TiC+3CO+10H_2$	1	1242.435–1.039T	1196
	2	1242.435–0.993T	1251
	3	1242.435–0.966T	1286
	4	1242.435–0.947T	1312

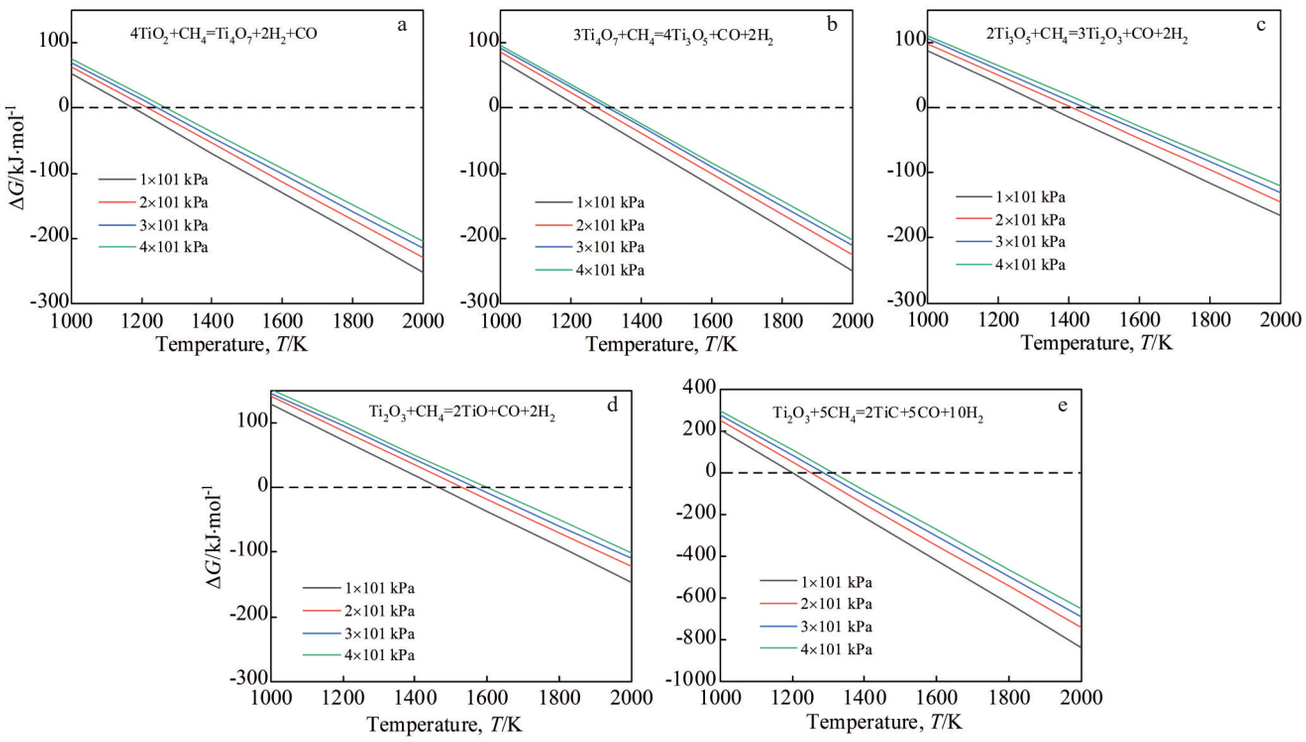

Fig.4 Relationships between Gibbs free energy change of titanium oxides and temperature in CH_4-H_2 gas mixture under varying system pressures

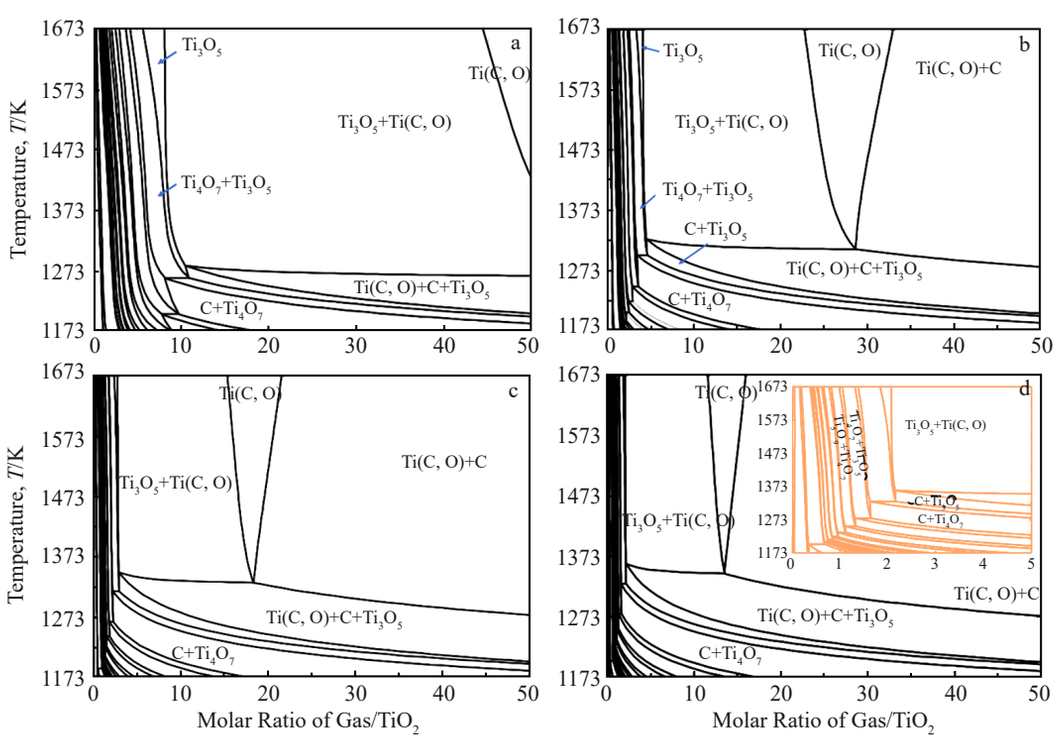

Fig.5 Equilibrium phase diagrams in different gas composition of TiO_2-(CH_4-H_2) systems: (a) TiO_2-$(CH_4)_{0.04}(H_2)_{0.96}$, (b) TiO_2-$(CH_4)_{0.08}(H_2)_{0.92}$, (c) TiO_2-$(CH_4)_{0.12}(H_2)_{0.88}$, and (d) TiO_2-$(CH_4)_{0.16}(H_2)_{0.84}$

in the phase equilibrium calculations. Once all titanium oxides in the system are transformed into the Ti(C, O) solid solution, TiO is further converted to TiC by CH_4, causing the molar fraction of TiC in the solid solution to increase with the rising gas content.

3.4 Change of reaction enthalpy

The equilibrium between TiO_2 and the CH_4-H_2 gas mixture in an open system is analyzed, with the calculation conditions detailed in Table 6. To achieve the complete carbonization of TiO_2, the reaction was divided into 1000 steps, where 0.1 mol

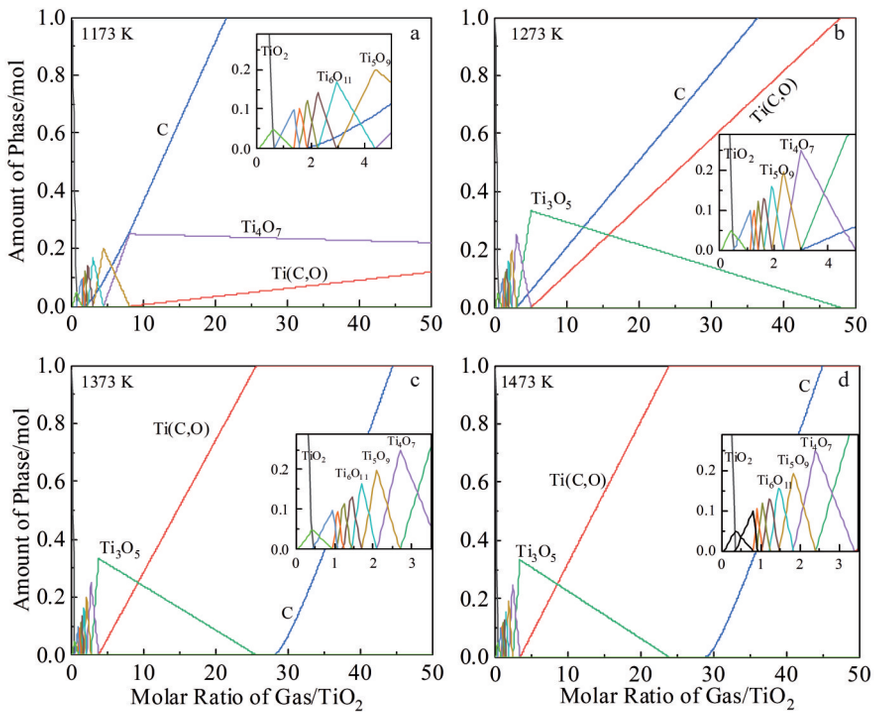

Fig.6 Solid phase composition at different temperatures in TiO_2-(8vol% CH_4-92vol% H_2) open system: (a) 1173 K, (b) 1273 K, (c) 1373 K, and (d) 1473 K

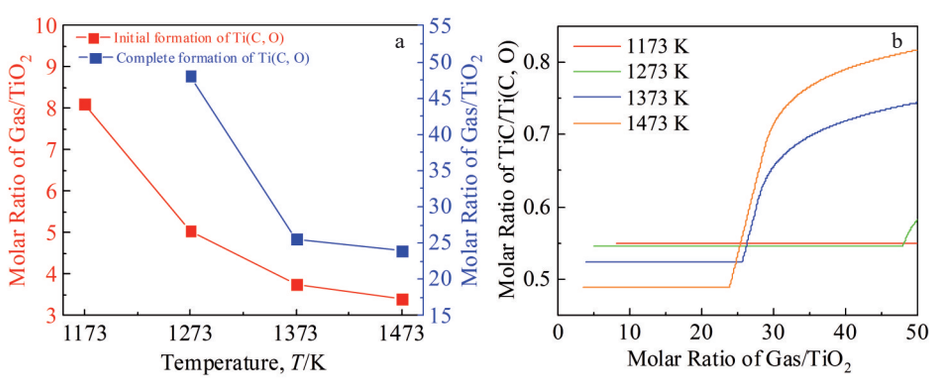

Fig.7 Initial and complete formation points of Ti(C, O) (a) and content variation of TiC in Ti(C, O) (b) in TiO_2-(8vol% CH_4-92vol% H_2) open system

Table 6 Calculation conditions of TiO_2 with CH_4-H_2 gas mixture in open system

No.	CH_4/%	H_2/%	T/℃	P_{total}/×101 kPa
1			1000	
2	8	92	1100	1
3			1200	

reactant gas was introduced in each step. The heat capacity data for each substance in the system are presented in Table 7, which were sourced from the FactSage 8.0 databases (FactPS and FToxid).

As illustrated in Table 8, the amount of gas required for the complete carbonization of 1 mol TiO_2 at 1000, 1100, and 1200 ℃ is 48.00, 25.75, and 24.00 mol, respectively. The energy consumption during the reaction process was calculated and is depicted in Fig. 8. This includes the reaction enthalpy of the system at the target temperature and the sensible heat required to heat the substances to the target temperature. The changes in reaction enthalpy at 1000, 1100, and 1200 ℃ are 787, 623, and 600 kJ, respectively, highlighting that the reduction process is endothermic.

In practical applications, reactants are typically preheated to a specific temperature using waste heat, which provides a

Table 7 Thermodynamic data of substances during the carbonitriding process of TiO_2

Substance	C_p/J·(mol·K)$^{-1}$
TiO_2	$77.83-3367841T^{-2}+4.0294\times10^{8}T^{-3}$
CH_4	$304.93-0.0188T-10143.98T^{-0.5}+110598.4T^{-1}-4193372T^{-2}$
H_2	$19.82+3\times10^{-3}T+1.43\times10^{-6}T^{2}+194.86T^{-0.5}-295179.9T^{-2}$
$Ti_{20}O_{39}$	$1609.77-2110.89T^{-0.5}-56404973T^{-2}+6.3025\times10^{9}T^{-3}$
$Ti_{10}O_{19}$	$831.4-2110.89T^{-0.5}-22726564T^{-2}+2.273\times10^{9}T^{-3}$
Ti_9O_{17}	$753.55-2110.89T^{-0.5}-19358722T^{-2}+1.87\times10^{9}T^{-3}$
Ti_8O_{15}	$675.71-2110.89T^{-0.5}-15990881T^{-2}+1.47\times10^{9}T^{-3}$
Ti_7O_{13}	$597.88-2110.89T^{-0.5}-12626040T^{-2}+1.06\times10^{9}T^{-3}$
Ti_6O_{11}	$520.04-2110.89T^{-0.5}-9255199.2T^{-2}+6.61\times10^{8}T^{-3}$
Ti_5O_9	$442.2-2110.89T^{-0.5}-5887358.3T^{-2}+2.58\times10^{8}T^{-3}$
Ti_4O_7	$364.37-2110.89T^{-0.5}-2519517.2T^{-2}+1.44\times10^{8}T^{-3}$
Ti_3O_5	$158.99+0.0502T$
Ti_2O_3	$169.96-750.22T^{-0.5}+1609648.9T^{-2}-1.56\times10^{9}T^{-3}$
TiO	$41.99+0.0178T-6.64\times10^{-8}T^{2}-654021.18T^{-2}$ $53.36+0.003T-6.4\times10^{-7}T^{2}-527047.2T^{-2}$ (298–900 K)
TiC	$53.35+0.0019T+5.45\times10^{-7}T^{2}-5210560T^{-2}$ (900–1155 K) $44.31+0.0098T-1.22\times10^{-6}T^{2}-2169880T^{-2}$ (1155–1941 K)
TiN	$70.28-0.0024T+1.22\times10^{-5}T^{2}-5877.49T^{-1}-664722.08T^{-2}$ (298–1100 K) $40.76+0.0098T+1693618T^{-2}$ (1100–3220 K)
H_2O	$25.78+0.015T-5.52\times10^{-7}T^{2}+1107.27T^{-1}-27999.3T^{-2}$ (298–1100 K)
H_2O	$53.15+1.61\times10^{-4}T-1486.84T^{-0.5}-83128.27T^{-1}+2.41\times10^{7}T^{-2}$ (1100–4000 K)
CO	$44.09+22893.91T^{-1}-11633086T^{-2}-687.27T^{-0.5}$
CO_2	$103.34-0.0047T-1748.29T^{-0.5}+11004.74T^{-1}-40249T^{-2}$
C	$61.18-0.008T-1024T^{-0.5}+825570T^{-2}-6604775.7T^{-3}$ (298–1000 K) $24.78+9.59\times10^{-4}T-39.69T^{-0.5}-2883408.3T^{-2}$ (1000–6000 K)

Table 8 Amount of gas required for complete carbonization of TiO_2 with CH_4-H_2 gas mixture

No.	CH_4/%	H_2/%	T/℃	Gas required/mol
1			1000	48
2	8	92	1100	25.75
3			1200	24

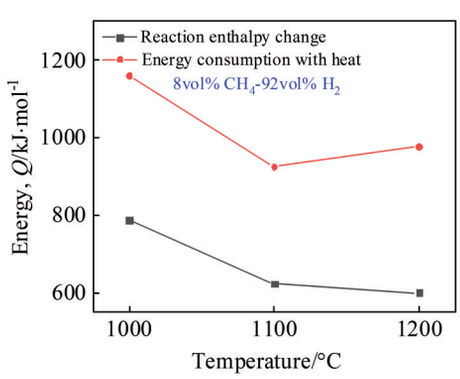

Fig.8 Energy consumption during the reduction process of TiO_2 in CH_4-H_2 gas mixture

portion of heat to the reaction system. Assuming that H_2 and solids are preheated to 900 ℃ while methane remains unheated due to low-temperature pyrolysis, the adjusted energy consumption is also presented in Fig. 8. The total energy required for the complete carbonization of 1 mol TiO_2 at 1000, 1100, and 1200 ℃ is 1159, 925, and 977 kJ, respectively. Under these conditions, the total energy consumption for producing 1 t of Ti(C, O) at 1100 ℃, considering raw material heating, is 12.17 GJ, which is equivalent to the energy of 415.39 kg standard coal.

4 Conclusions

1) Within the CH_4-H_2 system, the reaction between TiO_2 and H_2 is more difficult to initiate than that between TiO_2 and CH_4. Increasing the CH_4 concentration or raising the reaction temperature can decrease the total gas demand and heat required for the formation of Ti(C, O). Furthermore, the initial reaction temperature decreases with a reduction in partial pressure of gaseous products.

2) TiO_2 is initially transformed into the Magnéli phase, subsequently into the Ti_3O_5 phase, and ultimately into the solid solution phase Ti(C, O). Appropriately elevating the reaction temperature facilitates the formation of the Ti(C, O) solid solution, thereby reducing gas consumption and preventing excessive carbon deposition.

3) Under the conditions of 1100 ℃ and a gas mixture composed of 8vol% CH_4-92vol% H_2, the enthalpy change and total energy consumption for the complete carbonization of 1 mol of TiO_2 are 623 and 925 kJ, respectively.

References

1 González J, Mirza-Rosca J. *J Electroanal Chem*[J], 1999, 471(2): 109

2 Atapour M, Fathi M, Shamanian M. *Mater Corros*[J], 2012, 63(2): 134

3 Cui Yuwei, Chen Liangyu, Liu Xinxin. *Curr Nanosci*[J], 2021, 17(2): 241

4 Boffano P, Brucoli M, Rocchetti V. *J Maxillofac Oral Surg*[J], 2024, 23(6): 2169

5 Ji Min, Zhang Shuai, Qiu Jiajun *et al. J Mater Res Technol*[J], 2024, 33: 4105

6 Guo J L, Wang F, Liou J J *et al. Rare Metal Materials and Engineering*[J], 2024, 53(3): 617

7 Chen Song, Huang Sensen, Ma Yingjie *et al. Rare Metal Materials and Engineering*[J], 2024, 53(2): 435 (in Chinese)

8 Ma X L, Kazuhiro M, Shang Z F *et al. Rare Metal Materials and Engineering*[J], 2024, 53(4): 947

9 Elhadd A, Remero-Resendz L, Ross M *et al. J Mater Res Technol*[J], 2024, 33: 3550

10 Zhong Wen, Yu Kui, Shi Jipeng *et al. J Mater Res Technol*[J], 2024, 30: 3355

11 Niinomi M. *J Iron Steel Inst Jpn*[J], 2004; 90(7): 462

12 Fanning J. *J Mater Eng Perform*[J], 2005, 14(6): 686

13 Wu Xuanxuan, Dong Xianjuan, Xu Yong *et al. Rare Metal Materials and Engineering*[J], 2024, 53(5): 1409 (in Chinese)

14 Hunter M A. *Metallic Titanium*[M]. New York: Rensselaer Polytechnic Institute, 1911

15 Mohanty J, Rath P, Parmguru R *et al*. *Trans Indian Inst Met*[J], 2006, 59(1): 1

16 Ozge G, Rhmi U. *J Alloy Compd*[J], 2022, 929: 167262

17 Feng Qisheng, Lv Mingrui, Mao Lu *et al. Metals*[J], 2023, 13(2): 408

18 Kroll W. *Trans Electrochem*[J], 1940, 78: 35

19 Zhang Ying, Fang Zhigang, Sun Pei *et al. JOM*[J], 2017, 69(10): 1861

20 Kumar V, Gupta R, Prasad M *et al. J Mater Res*[J], 2021, 36(3): 689

21 Jackson M, Dring K. *Mater Sci Technol*[J], 2006, 22(8): 881

22 Zhang Wensheng, Zhu Zhaowu, Cheng Chuyong. *Hydrometallurgy*[J], 2011, 108(3–4): 177

23 Wu Enhui, Zhu Rong, Yang Shaoli *et al. Iron Steel Vanadium Titanium*[J], 2016, 37(1): 46 (in Chinese)

24 Qin Jie, Wang Yue, You Zhixiong *et al. J Mater Res Technol*[J], 2020, 9(3): 4272

25 Withers J C, Loutfy R O. *U S Patent.* WO2002019501A2[P]. 2005

26 Popov B, Kimble M, White R *et al*. *J Appl Electrochem*[J], 1991, 21(4): 351

27 Jiao Shuqiang, Zhu Hongmin. *J Mater Res*[J], 2011, 21(9): 2172

28 Jiao Shuqiang, Zhu Hongmin. *J Alloy Compd*[J], 2007, 438(1–2): 243

29 Ali M, Basu P. *J Alloy Compd*[J], 2010, 500(2): 220

30 Feng Xin, Bai Yujun, Lü Bo *et al. J Cryst Growth*[J], 2004, 264(1–3): 316

31 Feng Xin, Bai Yujun, Lü Bo *et al. Inorg Chem*[J], 2004, 43(12): 3558

32 Wang Liangbiao, Li Qianwen, Zhu Yongchun *et al*. *Int J Refract Met Hard Mat*[J], 2012, 31: 288

33 Zhang G Q, Ostrovski O. *Metall Mater Trans B-Proc Metall Mater Proc Sci*[J], 2000, 31(1): 129

34 Dang J, Fatollahi-Fard F, Pistorius P *et al*. *Metall Mater Trans B-Proc Metall Mater Proc Sci*[J], 2017, 48: 2440

35 Dewan M, Zhang G Q, Ostrovski O. *Metall Mater Trans B-Proc Metall Mater Proc Sci*[J], 2009, 40(1): 62

36 Fan Gangqiang, Dang Jie, Zhang Run *et al*. *Int J Energy Res*[J], 2020, 44(6): 4861

37 Fan Gangqiang, Hou Youling, Huang Dejun *et al. Int J Refract Met Hard Mat*[J], 2021, 101: 1056

38 Shadman Z. *Ind Eng Chem Res*[J], 1991, 30(9): 2080

39 Jones D. *Journal of Applied Chemistry and Biotechnology*[J], 1975, 25(8): 561

40 Sun K, Takahashi R, Yagi J. *ISIJ International*[J], 1992, 32(4): 496

41 Choi K, Jeon H, Lee S *et al. Metall Mater Trans B-Proc Metall Mater Proc Sci*[J], 2022, 53(1): 334

42 Zhang Run, Liu Dong, Fan Gangqiang *et al. Int J Energy Res*[J], 2019, 43(9): 4253

CH_4-H_2混合气体还原二氧化钛的热力学研究

田臻赟[1]，陈佳文[1]，张　润[1]，范刚强[1,2,3]，邱贵宝[1,4]

(1. 重庆大学 材料科学与工程学院，重庆 400044)

(2. 重庆望变电气(集团)股份有限公司，重庆 401254)

(3. 高性能取向电工钢重庆市重点实验室，重庆 401254)

(4. 重庆大学 重庆市钒钛冶金与新材料重点实验室，重庆 400044)

摘　要：针对钛及碳化钛制备这一全球关注的重要课题，开发了一种基于CH_4-H_2混合气体的新型TiO_2还原工艺，并对其中存在的热力学行为、相平衡和能耗进行了研究。结果表明，在CH_4-H_2混合气氛下，TiO_2的还原过程呈现出独特的逐步转化特征，其反应路径遵循从TiO_2到Ti(C, O)的演变规律，过程中可观察到Magnéli相（Ti_nO_{2n-1}）和Ti_3O_5等低价氧化物作为重要的中间相存在。与传统的纯CH_4还原体系相比，H_2的引入显著增加了反应难度，这一现象可能与H_2对表面碳沉积的抑制作用有关。在能量消耗方面，获得了具有重要指导意义的数据：在标准条件下，1000 ℃时完全碳化反应的能耗为1159 kJ/mol，当温度升至1100 ℃时能耗显著降低至925 kJ/mol，而继续升温至1200 ℃时却出现能耗回升至977 kJ/mol的反常现象，这可能与高温下气相平衡的移动和副反应增加有关。

关键词：TiO_2；TiC_xO_y；还原碳化；热力学行为；能量消耗

作者简介：田臻赟，男，1997年生，博士生，重庆大学材料与工程学院，重庆 400044，E-mail：tianzhenyun@cqu.edu.cn